Virology 383 (2009) 248–260

Contents lists available at ScienceDirect

Virology

journal homepage: www.elsevier.com/locate/yviro

Evidence for alternate states of *Cucumber mosaic virus* replicase assembly in positive- and negative-strand RNA synthesis

Jang-Kyun Seo [a,b], Sun-Jung Kwon [c], Hong-Soo Choi [d], Kook-Hyung Kim [a,b,c,*]

[a] *Department of Agricultural Biotechnology, College of Agriculture and Life Sciences, Seoul National University, Seoul 151-921, South Korea*
[b] *Institute of Molecular Biology and Genetics, Seoul National University, Seoul, South Korea*
[c] *Research Institute for Agriculture and Life Sciences, Seoul National University, Seoul 151-921, South Korea*
[d] *National Institute of Agricultural Science and Technology, Rural Development Administration, Suwon 441-707, South Korea*

ARTICLE INFO

Article history:
Received 4 July 2008
Returned to author for revision 30 August 2008
Accepted 21 October 2008
Available online 20 November 2008

Keywords:
CMV
Replication
Temporal regulation
Replicase components

ABSTRACT

Cucumber mosaic virus (CMV) encodes two viral replication proteins, 1a and 2a. Accumulating evidence implies that different aspects of 1a–2a interaction in replication complex assembly are involved in the regulation of virus replication. To further investigate CMV replicase assembly and to dissect the involvement of replicase activities in negative- and positive-strand synthesis, we transiently expressed CMV RNAs and/or proteins in *Nicotiana benthamiana* leaves using a DNA or RNA-mediated expression system. Surprisingly, we found that, even in the absence of 1a, 2a is capable of synthesizing positive-strand RNAs, while 1a and 2a are both required for negative-strand synthesis. We also report evidence that 1a capping activities function independently of 2a. Moreover, using 1a mutants, we show that capping activities of 1a are crucial for viral translation but not for RNA transcription. These results support the concept that two or more alternate states of replicase assembly are involved in CMV replication.

Introduction

Programmed regulation of viral replication is essential for successful infection by a positive-strand RNA virus. In the early phase of virus infection, viral genomic RNAs are translated into the proteins involved in RNA replication, which include an RNA-dependent RNA polymerase (RdRp) and additional replicase proteins. These proteins constitute the viral replication complex in association with some host proteins, and act to recruit viral genomic RNAs as templates for the synthesis of negative-strand RNA. At some point, negative-strand synthesis ceases and the viral replication complex uses negative-strand RNAs as templates for the synthesis of new genomic positive-strand RNA and, for several virus groups, subgenomic RNA. These events are likely complex reactions, because replication is temporally regulated during the viral life cycle by both viral- and host-encoded proteins.

Cucumber mosaic virus (CMV) is a member of the alphavirus-like superfamily of plant and animal positive-strand RNA viruses. The CMV genome consists of three 5′-capped positive-strand RNAs (Symons, 1975). RNA3 is bicistronic, encoding two proteins involved in the movement of the virus, while RNA 1 and 2 encode the replication proteins 1a (110 kDa) and 2a (97 kDa), respectively (Palukaitis and Garcia-Arenal, 2003). RNA2 also encodes the multifunctional protein 2b, which is not involved in virus replication (Ding et al., 1996). All members of the alphavirus-like superfamily contain three homologous domains in their RNA replication proteins, which have similarities to RNA-capping enzyme, helicase, and RdRp, respectively (Koonin and Dolja, 1993). For different family members, these three conserved domains are differently organized on a single protein or among two or more separate proteins (van der Heijden and Bol, 2002). In CMV, the N-terminal half of 1a contains a methyltransferase-like domain for RNA capping, and the C-terminal half has homology to viral helicases (Palukaitis and Garcia-Arenal, 2003). CMV 2a contains core RdRp activity, which is presumably required for all steps of RNA synthesis (van der Heijden and Bol, 2002). 1a and 2a have been intensively studied in *Brome mosaic virus* (BMV), which is taxonomically closely related to CMV. 1a and 2a interact *in vitro* (Kao et al., 1992) and copurify with an active RdRp fraction from infected tissues (Kao et al., 1992; Quadt and Jaspars, 1990). Several studies have demonstrated that all three conserved domains are required for complete RNA replication and that interaction between 1a and 2a is important for the formation of a functional replicase complex for some steps of replication (Ahola et al., 2000; Dinant et al., 1993; Kao and Ahlquist, 1992; Kroner et al., 1990). However, it remains unclear whether 1a and 2a function separately or by forming a complex in each replication step; or whether 1a and 2a are both required for the synthesis of negative-strand, positive-strand, and subgenomic RNAs.

Accumulating evidence suggests that different sets or modes of 1a–2a interaction are involved in the replication cycle. For example, heterologous combinations of 1a and 2a protein of BMV and *Cowpea chlorotic mottle virus* (CCMV) have different abilities to support positive- and negative-strand accumulation (Allison et al., 1988;

* Corresponding author. Fax: +82 2 873 2317.
E-mail address: kookkim@snu.ac.kr (K.-H. Kim).

0042-6822/$ – see front matter © 2008 Elsevier Inc. All rights reserved.
doi:10.1016/j.virol.2008.10.033

Dinant et al., 1993). CCMV 1a and BMV 2a synthesize no detectable BMV RNA3, while BMV 1a and CCMV 2a direct negative-strand BMV RNA3 accumulation at 50% of the wild-type (wt) level and positive-strand BMV RNA3 accumulation at 3% of the wt level (Dinant et al., 1993). In addition, 1a is more abundant than 2a in purified RdRp (Hayes and Buck, 1990; Schwartz et al., 2002), although 2a accumulates in infected tissues at levels higher than 1a (Cillo et al., 2002; Gal-On et al., 1994). Furthermore, free 2a, which is not associated with 1a, is present in the cytoplasm of infected cells, while 1a is entirely membrane-associated (Gal-On et al., 2000; Restrepo-Hartwig and Ahlquist, 1999). Recent work shows that phosphorylation of CMV 2a catalyzed by host cellular kinases inhibits the interaction between 1a and 2a, suggesting a regulatory role for phosphorylation in the formation of the replicase complex (Kim et al., 2002).

To further examine the roles of 1a and 2a in CMV replication and to characterize the replication complex involved in negative- and positive-strand synthesis, we developed a DNA- and RNA-mediated transient expression system. Using this system, we found that 2a alone can synthesize positive-strand and subgenomic RNAs from negative-strand RNA templates. We also showed that 1a processes capping of positive-strand RNA despite the absence of 2a. Moreover, we showed that capping activities of 1a function independently of helicase activity in the capping reaction. These results support the idea that positive-strand RNA replication is regulated by altering interactions among the components of the replicase complex. A model for the temporal regulation of negative- and positive-strand RNA synthesis is discussed.

Results

2a supports positive-strand and subgenomic RNA synthesis in the absence of 1a

We infected *Nicotiana benthamiana* with T-DNA-based clones encoding CMV cDNAs under the control of the 35S promoter of *Cauliflower mosaic virus* (CaMV) using an *Agrobacterium*-mediated system (Fig. 1). An advantage of this system is that the desired set of

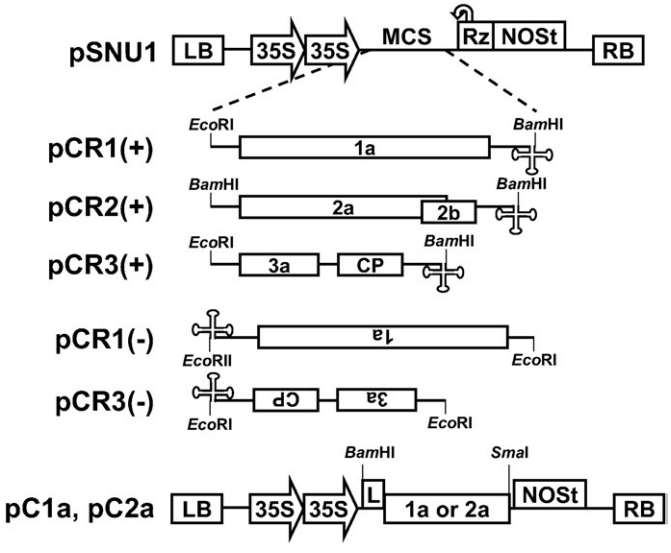

Fig. 1. Schematic representation of the T-DNA vector, pSNU1, and CMV cDNA constructs. The pSNU1 vector contains, in sequential order, a left border of T-DNA (LB), a double 35S promoter (35S), multiple cloning site (MCS), a *cis*-cleaving ribozyme sequence (Rz), a NOS terminator (NOSt), and a right border of T-DNA (RB). The constructs were named according to the molecule produced upon transient expression: for example, pCR1(+) and pCR3(−) express R1(+) (positive-strand RNA1) and R3(−) (negative-strand RNA3), respectively. pC1a and pC2a expressing CMV 1a and 2a, respectively, were modified by adding the tobacco etch virus leader sequence (L) and excluding an Rz cassette based on pSNU1. The restriction enzyme cleavage sites used to make the constructs are shown.

CMV RNAs and proteins can be consistently expressed independently of viral replication. All plants infiltrated with a mixture of *Agrobacterium* cultures containing pCR1(+), pCR2(+), and either pCR3(+) or pCR3(−) showed typical CMV-induced symptoms of stunting and distortion of the leaves, demonstrating that CMV RNAs transiently expressed from agroinfiltrated plasmids were fully infectious (data not shown).

To determine whether 1a is required for negative- or positive-strand synthesis, or for both, various combinations of CMV RNAs were transiently expressed in plants by agroinfiltration. At 3 days post-infiltration (dpi), leaf samples were collected and processed for analysis of positive- or negative-strand RNA3 accumulation using strand-specific reverse transcription (RT)-PCR. Since false priming of cDNA synthesis could occur in the RT reaction (Lanford et al., 1994), we developed a strand-specific RT-PCR capable of accurately discriminating between positive- and negative-strand RNA using tagged primers that contain non-CMV sequences at the 5′ end. The specificity and sensitivity of this strand-specific RT-PCR was verified using synthetic positive- and negative-strand CMV RNAs as references (data not shown). When this strand-specific RT-PCR was used for analysis of CMV replication, no PCR signal was observed in plants receiving pCR3(+), pCR3(−), or pCR1(−) alone as negative controls, demonstrating that non-specific RNA or DNA was not amplified (Fig. 2A, lanes 3, 9, and 15). First, we tested whether 1a is crucial for negative-strand synthesis. *Agrobacterium* cultures harboring pCR1(+) and/or pCR2(+) were mixed with *Agrobacterium* cultures transformed with pCR3(+) and then infiltrated into *N. benthamiana* leaves. As expected, plants infiltrated with pCR2(+) and pCR3(+) did not accumulate any detectable negative-strand RNA3, while accumulation of negative-strand RNA was detected in plants coinfiltrated with pCR2(+) and pCR3(+) together with pCR1(+) (Fig. 2A, lanes 1–6). These results indicated that 1a activities are crucial for negative-strand synthesis, consistent with those reported previously for BMV replication (Ahola et al., 2000; Gopinath et al., 2005). Next, we tested whether 1a is necessary for positive-strand synthesis from negative-strand templates. Plants were infiltrated with a mixture of *Agrobacterium* cultures containing pCR3(−) and either pCR2(+) or pCR1(+) and pCR2(+). Surprisingly, we detected the accumulation of positive-strand RNA in plants infiltrated with pCR2(+) and pCR3(−) as well as plants infiltrated with pCR1(+), pCR2(+), and pCR3(−) (Fig. 2A, lanes 7–12). Moreover, when plants were infiltrated with pCR1(−) and pCR2(+), accumulation of positive-strand RNA1 was detected, while negative controls showed no PCR product (Fig. 2A, lanes 13–18). These results were unexpected since previous studies suggested that both 1a and 2a are necessary for complete RNA replication and that interactions between 1a and 2a are important for virus replication (Ahola et al., 2000; Dinant et al., 1993; Kroner et al., 1990).

To confirm these strand-specific RT-PCR results, Northern blot analysis was performed using strand-specific probes. Despite extensive efforts, we could not demonstrate the accumulation of positive-strand RNA in the absence of RNA1 when we carried out Northern blotting using total RNA prepared from the *Agrobacterium*-mediated system because Northern blotting is, in general, less sensitive than RT-PCR. In addition, when we performed Northern blotting to detect negative-strand templates supplied by agroinfiltration, we could detect only very faint band for negative-strand templates in our experimental condition (data not shown). In similar experiments performed by other research groups, none or very faint band for BMV RNA3 transcripts singly expressed in plants by agroinfiltration was detected by northern blotting (Annamalai and Rao, 2005; Gopinath et al., 2005; Gopinath and Kao, 2007). Moreover, positive-strand RNAs synthesized by 2a alone are presumed to lack the cap-structure at the 5′ ends since capping activities for CMV RNA capping are conserved in 1a proteins. Actually, uncapped positive-strand RNAs produced by BMV defective in capping activities are much less stable than capped RNA and easily degraded by cellular nucleases (Ahola et al., 2000). Thus, it seems likely that positive-strand RNAs synthesized by 2a alone in agroinfiltration

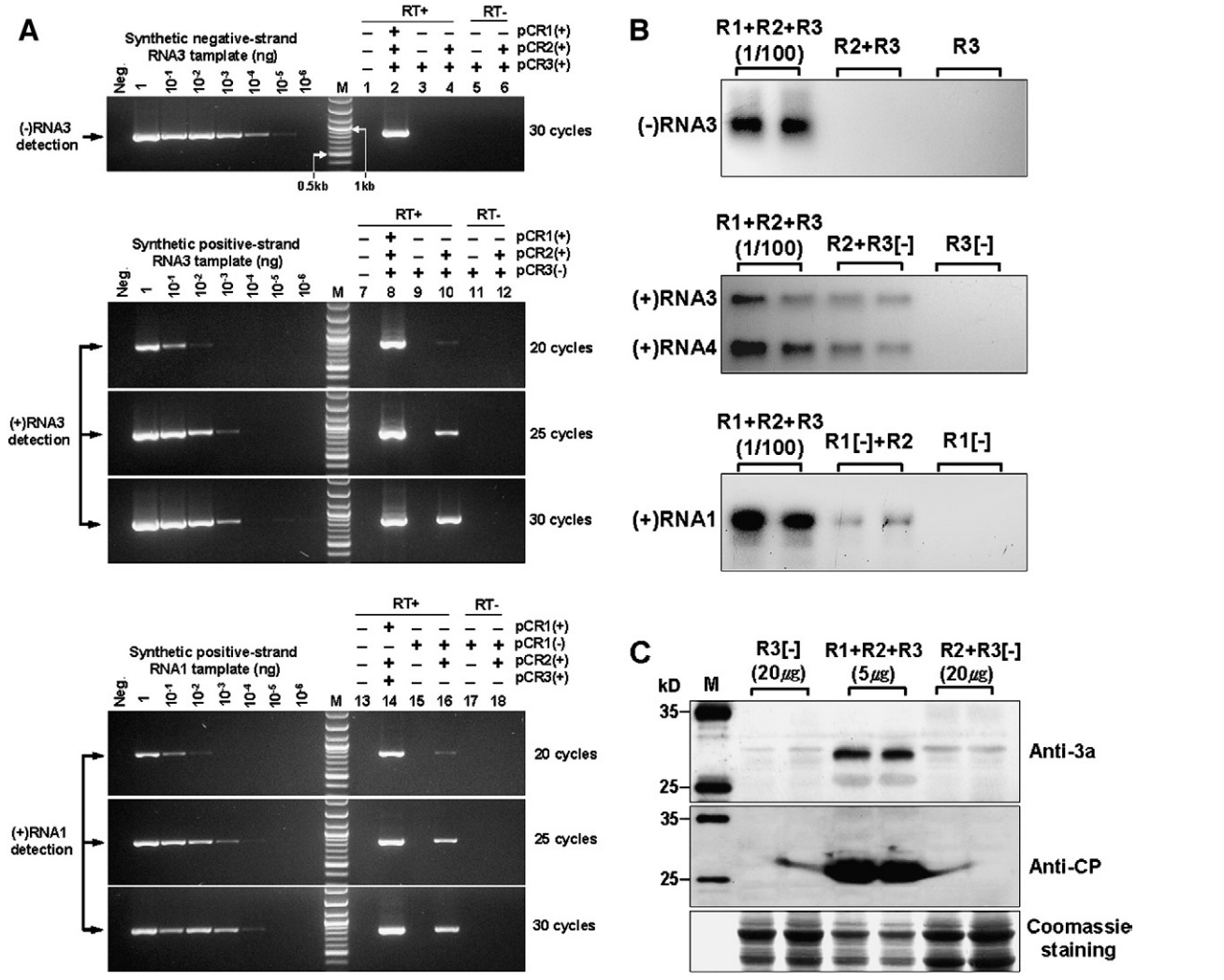

Fig. 2. Detection of positive- or negative-strand RNA accumulation and viral proteins in plants transiently expressing various combinations of CMV RNAs. (A) Strand-specific RT-PCR analysis. *N. benthamiana* leaves were agroinfiltrated with the following combinations: pCR1(+) + pCR2(+) + pCR3(+) (lane 2 and 14), pCR3(+) (lane 3), pCR2(+) + pCR3(+) (lane 4), pCR1(+) + pCR2(+) + pCR3(−) (lane 8), pCR3(−) (lane 9), pCR2(+) + pCR3(−) (lane 10), pCR1(−) (lane 15), and pCR1(−) + pCR2(+) (lane 16). Total RNA was extracted from infiltrated leaves and subjected to strand-specific RT-PCR for 20, 25, or 30 cycles using appropriate pairs of primers as described in the Materials and methods. Lanes 5, 6, 11, 12, 17, and 18 are reverse transcription negative controls for lanes 3, 4, 9, 10, 15, and 16, respectively. Lanes 1, 7, and 13 are RT-PCR negative controls for each primer pair. To assess the sensitivity of the strand-specific RT-PCR, ten-fold serially diluted synthetic CMV RNAs as references (ranging from 1 to 10^{-6} ng) were mixed with 1 μg of *N. benthamiana* total RNA and subjected to the strand-specific RT-PCR. Lane M contains 2-log ladder DNA marker (NEB, USA). Arrows indicate the expected PCR products. (B) Northern blot analysis. *N. benthamiana* leaves were inoculated with indicated combinations of capped transcripts, as shown at the top of each image. Total RNA was independently extracted from two inoculated leaves and processed for Northern blotting using strand-specific probes to detect positive or negative-strand RNAs as indicated on the left. (C) Western blot analysis. *N. benthamiana* leaves were inoculated with indicated combinations of capped transcripts, as shown at the top of image. Total protein was independently extracted from two inoculated leaves and subjected to immunoblot analysis with antibodies against CMV 3a or CP. Molecular weight markers are indicated on the left. Coomassie blue stained gel is shown below blots as a loading control.

system accumulate to undetectable level for northern blotting. Hence, we carried out Northern blotting by preparing total RNA from the *in vitro* transcribed RNA-based inoculation system. Positive- and negative-strand CMV RNA transcripts were produced by *in vitro* transcription using T7 RNA polymerase. All transcripts were capped by including synthetic GpppG in the transcription reaction to improve the translatability and stability of transcripts. Each transcript was named using the CMV RNA from which it was derived and a symbol indicating whether it was a positive-[+] or a negative-[−] strand.

To examine the synthesis of positive- or negative-strand RNA in the absence of RNA1, various mixtures of 10 μg of CMV RNA transcripts were mechanically inoculated into *N. benthamiana* leaves. All plants inoculated with a mixture of R1[+], R2[+], and either R3[+] or R3[−] transcripts developed typical CMV-induced symptoms (data not shown). At 2 days after inoculation, total RNA was extracted from inoculated leaves and subjected to Northern blotting using probes specific for positive- or negative-strand RNA. In plants inoculated with a mixture of R1[+], R2[+], and R3[+] transcripts, large amounts of negative-strand RNA3 and positive-strand RNA3 and RNA4 accumulated, whereas in the absence of R1[+] transcripts, there was no detectable negative-strand RNA3 (Fig. 2B). In plants inoculated with a mixture of R2[+], and R3[−] transcripts, low but significant synthesis of positive-strand RNA3 and RNA4 was detected (Fig. 2B). In repeated experiments, accumulation of RNA3 and RNA4 was approximately 0.5–1% of that in plants inoculated with a mixture of R1[+], R2[+], and R3[−] transcripts. Moreover, accumulation of positive-strand RNA1 was observed after inoculation with R1[−] and R2[+] transcripts (Fig. 2B). The accumulation of RNA1 was slight but clearly exceeded the amount resulting from inoculation with only R1[−]. However, comparison of viral RNA accumulation level in the absence and presence of 1a is not absolute since, in complete RNA replication, negative-strand and positive-strand progeny RNAs are used as templates for each other, and this amplifies viral RNAs by geometric progression, while 2a alone can only synthesize positive-strand from negative-strand, namely, positive-strand increases linearly in the absence of 1a. Moreover, none of the plants inoculated with either a

mixture of R2[+] and R3[−] transcripts or a mixture of R1[−] and R2[+] transcripts developed symptoms over a period of 3 weeks following the inoculation, indicating these plants were not contaminated with wt CMV. The leaf samples inoculated with a mixture of R2[+] and R3[−] transcripts were also analyzed by western blotting to examine whether CMV 3a and CP accumulate. In plants inoculated with a mixture of R1[+], R2[+], and R3[+] transcripts, we detected CMV 3a and large amounts of CP, whereas in plants inoculated with a mixture of R2 [+] and R3[−] transcripts, neither 3a nor CP was detected despite the accumulation of positive-strand RNA3 and RNA4 (Fig. 2C). Our Northern blot results are consistent with those of the strand-specific RT-PCR. Therefore, in the absence of 1a, 2a is capable of synthesizing positive-strand RNAs from the negative-strand templates, although 1a is obviously required for negative-strand synthesis.

The synthesis of positive-strand RNA is specifically regulated by 2a

The stem-loop C (SLC) elements in the 3′-terminal tRNA-like structure of positive-strand CMV RNAs have been identified as the core promoters required for replicase binding and initiation of negative-strand RNA synthesis (Boccard and Baulcombe, 1993; Sivakumaran et al., 2000). Moreover, the core promoters directing positive-strand RNA synthesis are located near the 3′ terminus of negative-strand CMV RNAs (Choi et al., 2004; Palukaitis and Garcia-Arenal, 2003; Sivakumaran et al., 1999, 2000; Sivakumaran and Kao, 1999). Sequences necessary for promoting the synthesis of subgenomic RNA4 and RNA4A have also been identified (Chen et al., 2000; Sivakumaran et al., 2002). Based on these previously characterized core promoters, we constructed CMV RNA3 deletion mutants, which were truncated at the 5′ or 3′ terminus containing the core promoter for positive- or negative-strand synthesis, respectively (Fig. 3A). Using these mutants, we investigated whether the synthesis of positive-strand RNA from negative-strand template is specifically regulated by 2a in the absence of 1a. *Agrobacterium* cultures containing pCR2(+) were mixed with *Agrobacterium* cultures transformed with pCR3(−), pCR3(−)Δ3, or pCR3(−)Δ5, and then infiltrated into *N. benthamiana* leaves. At 2 dpi, accumulation of positive-strand CMV RNA3 was analyzed using strand-specific RT-PCR. When pCR3(−)Δ3 lacking the core promoter for positive-strand synthesis was infiltrated with pCR2 (+), the accumulation of positive-strand RNA3 was not detected (Fig.

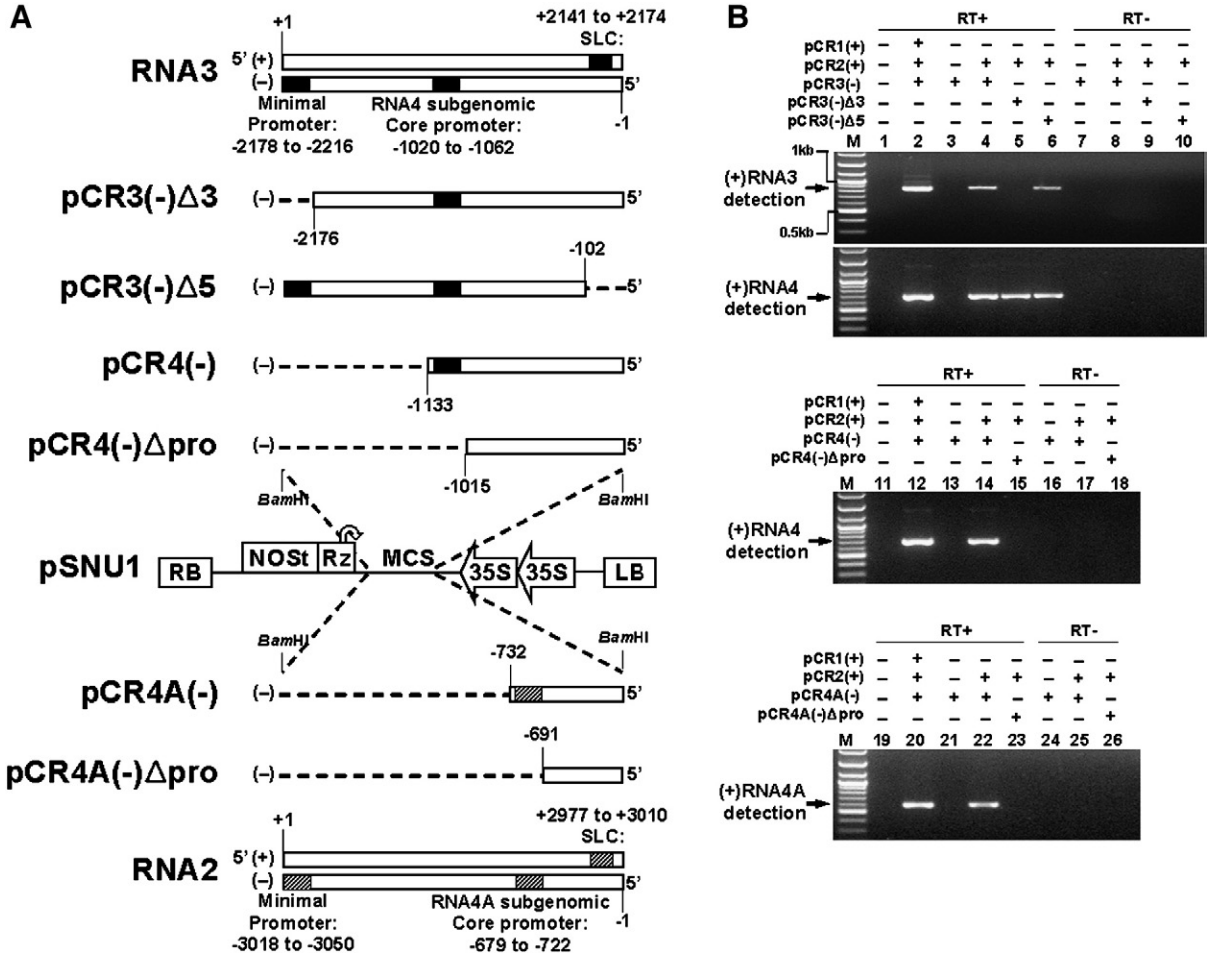

Fig. 3. Effects of CMV *cis*-acting sequences on positive-strand RNA synthesis in plants. (A) Schematic representation of *cis*-acting sequences in CMV RNA2, RNA3, and 5′- or 3′-terminus deleted mutant clones. Locations of cis-acting sequences are denoted by shaded boxes (RNA3) or hatched boxes (RNA2). Positive- and negative-strands are denoted with "(+)" or "(−)". pCR3(−)Δ3 expresses negative-strand RNA3 containing the sequence from nucleotide (nt) 1 to 2176. pCR3(−)Δ5 expresses negative-strand RNA3 containing the sequence from nt 102 to 2216. pCR4(−) expresses negative-strand RNA3 containing the sequence from nt 1 to 1133. pCR4(−)Δpro expresses negative-strand RNA3 containing the sequence from nt 1 to 1015. pCR4A(−) expresses negative-strand RNA2 containing the sequence from nt 1 to 732. pCR4A(−)Δpro expresses negative-strand RNA2 containing the sequence from nt 1 to 691. (B) Strand-specific RT-PCR for detection of positive-strand RNA accumulation in plants infiltrated with the CMV RNA deletion mutants. *N. benthamiana* leaves were agroinfiltrated with the following combinations: pCR1(+) + pCR2(+) + pCR3(−) (lane 2), pCR3(−) (lane 3), pCR2(+) + pCR3(−) (lane 4), pCR2(+) + pCR3(−)Δ3 (lane 5), pCR2(+) + pCR3(−)Δ5 (lane 6), pCR1(+) + pCR2 (+) + pCR4(−) (lane 12), pCR4(−) (lane 13), pCR2(+) + pCR4(−) (lane 14), pCR2(+) + pCR4(−)Δpro (lane 15), pCR1(+) + pCR2(+) + pCR4A(−) (lane 20), pCR4A(−) (lane 21), pCR2(+) + pCR4A (−) (lane 22), pCR2(+) + pCR4(−)Δpro (lane 23). Total RNA was isolated from infiltrated leaves and subjected to strand-specific RT-PCR for 30 cycles with appropriate pairs of primers as described in the Materials and methods. Lanes 7, 8, 9, 10, 16, 17, 18, 24, 25, and 26 are reverse-transcription negative controls for lanes 3, 4, 5, 6, 13, 14, 15, 21, 22, and 23. Lanes 1, 11, and 19 are RT-PCR negative controls for each primer pair. Lane M contains 2-log ladder DNA marker. Arrows indicate the expected PCR products.

3B, lane 5). In contrast, we detected the synthesis of positive-strand RNA3 in plants infiltrated with pCR2(+) and pCR3(−)Δ5 (Fig. 3B, lane 6). These results suggest that 2a alone can recognize and bind to the core promoter in the 3′ terminus of negative-strand RNA for initiation of positive-strand RNA synthesis, while the sequence complementary to SLC in the 5′ terminus of the negative-strand is not required for positive-strand RNA synthesis. In addition, when we carried out strand-specific RT-PCR for detection of subgenomic RNA4, we detected the accumulation of subgenomic RNA4 in plants infiltrated with pCR2(+) and pCR3(−)Δ3 as well as plants infiltrated with pC2a and pCR3(−)Δ5 (Fig. 3B, lanes 5 and 6). Thus, to test whether 2a could recognize the subgenomic promoters and regulate accumulation of subgenomic RNA4 and RNA4A in the absence of 1a, we designed partial negative-strand RNA3 and RNA2 constructs either containing or lacking a subgenomic minimal promoter sequence (Fig. 3A). When plants infiltrated with pCR2(+) and either pCR4(−) or pCR4A(−) were analyzed by strand-specific RT-PCR, the accumulation of subgenomic RNA4 and RNA4A was detected (Fig. 3B, lanes 14 and 22). In contrast, when pCR4(−)Δpro or pCR4A(−)Δpro lacking the core promoter for subgenomic RNA synthesis was infiltrated with pCR2(+), the accumulation of positive-strand RNA3 was not detected (Fig. 3B, lanes 15 and 23). Therefore, 2a alone can direct the synthesis of subgenomic RNAs by recognizing the subgenomic promoters.

Comparison of 2a-directed positive-strand synthesis activity in the absence and/or presence of 1a and the accumulation kinetics of CMV RNA in plants

To compare the activity of 2a-directed positive-strand RNA synthesis in the absence and presence of 1a using negative-strands as templates, plants were agroinfiltrated with pC1a and/or pC2a simultaneously with pCR3(−)Δ5, which produces nonreplicatable negative-strand RNA3 due to deletion of the complementary stem-loop C (SLC) region (Fig. 3A). Total RNA was extracted at 24, 48, 72, and 96 h post-infiltration (hpi) to analyze the kinetics of positive-strand RNA accumulation. The accumulation of positive-strand RNA3 and subgenomic RNA4 was quantified by real-time RT-PCR using primers specifically designed for positive-strand RNA detection. As shown in Fig. 4 (panels A and B), the rate of positive-strand accumulation in plants infiltrated with pC1a, pC2a, and pCR3(−)Δ5 was nearly linear until 96 hpi, reflecting the fact that synthesis of positive-strand RNA3 was maintained constantly without viral replication. Moreover, the rate of accumulation of positive-strand RNA3 in the absence of 1a was similar to that after infiltration of pC1a, pC2a, and pCR3(−)Δ5 until 48 hpi (Fig. 4A). However, at 72 and 96 hpi, positive-strand RNA3 accumulation in the absence of 1a was reduced to approximately 64% and 61% of that in the presence of 1a, respectively (Fig. 4A). This is likely due to the extended half-life of RNA3 transcripts, since 1a increases *in vivo* stability of positive-strand RNA3. As shown previously (Janda and Ahlquist, 1998), expressing 1a with RNA3 in yeast had a dramatic effect on RNA3 stability. RNA3 degradation in yeast expressing 1a was slowed 20- to 40-fold compared to that of yeast lacking 1a, yielding a half-life greater than 3 h. A similar pattern of accumulation was observed when real-time RT-PCR was carried out to quantify the accumulation of both positive-strand RNA3 and RNA4 (Fig. 4B). These results show that 2a activity associated with the synthesis of positive-strand RNA from negative-strand template is not significantly affected by 1a activities.

Next, we analyzed the accumulation kinetics of CMV positive- and negative-strand RNA in plants infected with CMV to examine whether the synthesis of positive and negative strands is differently regulated. *N. benthamiana* plants were agroinfiltrated with pCR1(+), pCR2(+), and

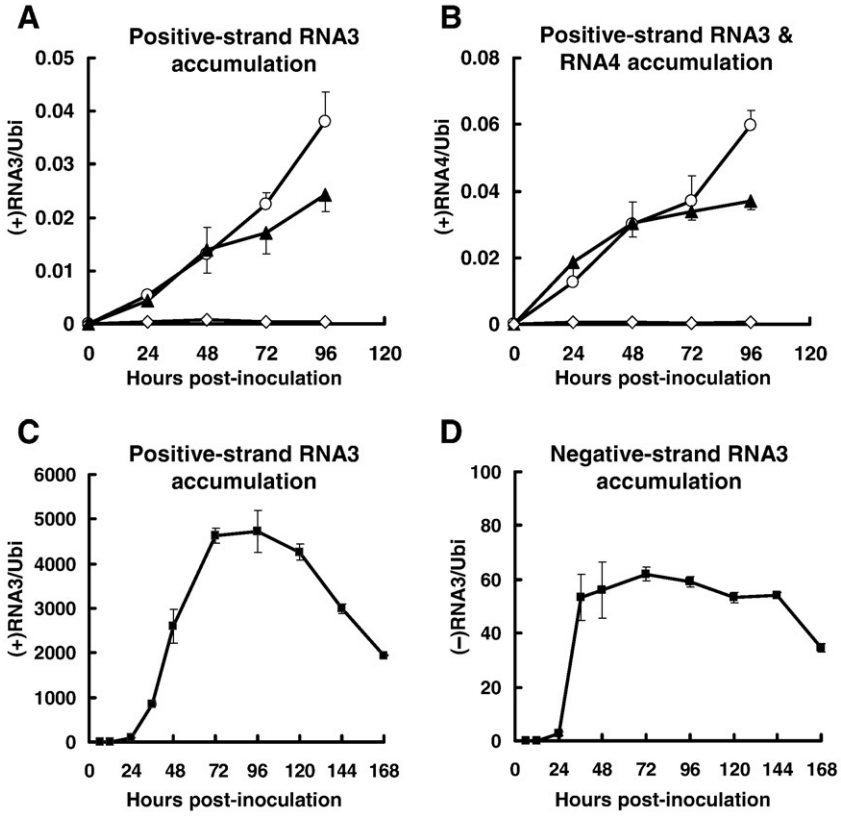

Fig. 4. Time course of CMV RNA accumulation in plants. *N. benthamiana* leaves were agroinfiltrated with the following combinations: pC1a + pC2a + pCR3(−)Δ5 (○), pC2a + pCR3(−)Δ5 (▲), pCR3(−)Δ5 alone (◊), and pCR1(+) + pCR2(+) + pCR3(+) (•). Total RNA was extracted form infiltrated leaves at the times indicated on the horizontal axes. Accumulation of positive-strand RNA3 (A and C), both positive-strand RNA3 and RNA4 (B), or negative-strand RNA3 (D) was quantified by real-time RT-PCR as described in the Materials and methods. Values are shown as the ratio of the accumulation level of CMV RNAs to the corresponding *ubiquitin* gene±SEM from three independent experiments.

pCR3(+). Total RNA was extracted from infiltrated leaves at different times post-infiltration and subjected to real-time RT-PCR to analyze the kinetics of positive- and negative-strand RNA accumulation. Insignificant levels of positive- and negative RNA3 continued to accumulate through 24 hpi, and then the majority of positive-strand accumulation occurred from 24 to 72 hpi (Figs. 4C and D). However, a different pattern of negative-strand accumulation was observed. The majority of negative-strand accumulation occurred during 24 to 36 hpi and the level was maintained to 144 hpi (Fig. 4D). This result reveals that the switching of CMV RNA replication from negative-strand synthesis to positive-strand synthesis occurred around 36 hpi in plants.

Positive-strand RNAs synthesized by 2a alone are not translated detectably

To address whether positive-strand RNAs synthesized by 2a alone are functional for translation, we replaced the 3a coding sequences in pCR3(+) and pCR3(−) with a sequence coding for green fluorescent protein (GFP; Fig. 5A). The resulting plasmids were named pCR3(+)GFP and pCR3(−)GFP, respectively. In the case of pCR3(−)GFP, GFP can be translated from complementary positive-strand RNA synthesized by CMV replicase from transcripts using pCR3(−)GFP as a template. To ensure that pCR3(+)GFP produces detectable levels of GFP, this construct was singly agroinfiltrated into *N. benthamiana* leaves. Under this condition, GFP fluorescence was observed in infiltrated leaves within 48 hpi (data not shown). Therefore, we examined the translatability of positive-strand RNAs synthesized by 2a alone using this agroinfiltration system by coexpressing pCR3(−)GFP with 1a, 2a, or both proteins. At 3 dpi, we could detect high levels of GFP fluorescence from plants coinfiltrated with pCR3(−)GFP together with pC1a and pC2a as well as plants infiltrated with pCR(+)GFP alone (Fig. 5B). However, plants infiltrated to express either 1a or 2a alone had no GFP signal (Fig. 5B). These results reveal that positive-strand RNAs synthesized by 2a in the absence of 1a are not detectably translated under these conditions. In fact, CMV genomic positive-strand RNAs have a m^7G cap structure at their 5′ ends similar to most cellular mRNAs (Symons, 1975). One of the most important functions of the cap is to allow translatability (Gallie, 1991). Since cellular mRNAs gain access to the ribosome for translation via a cap-binding protein that recognizes the cap, if there is no cap, the cap-binding protein cannot bind and the mRNA is very poorly translated (Sonenberg et al., 1980). In CMV, 1a has activities similar to those of the *Sindbis virus* (SIN) nsP1 protein, which include methyltransferase and possibly guanylyltransferase activities, and hence are presumed to provide the 5′ cap structure to viral genomic RNAs (van der Heijden and Bol, 2002). Thus it seems likely that 2a alone, without 1a activities, is incapable of producing translatable RNAs because they will lack the cap structure.

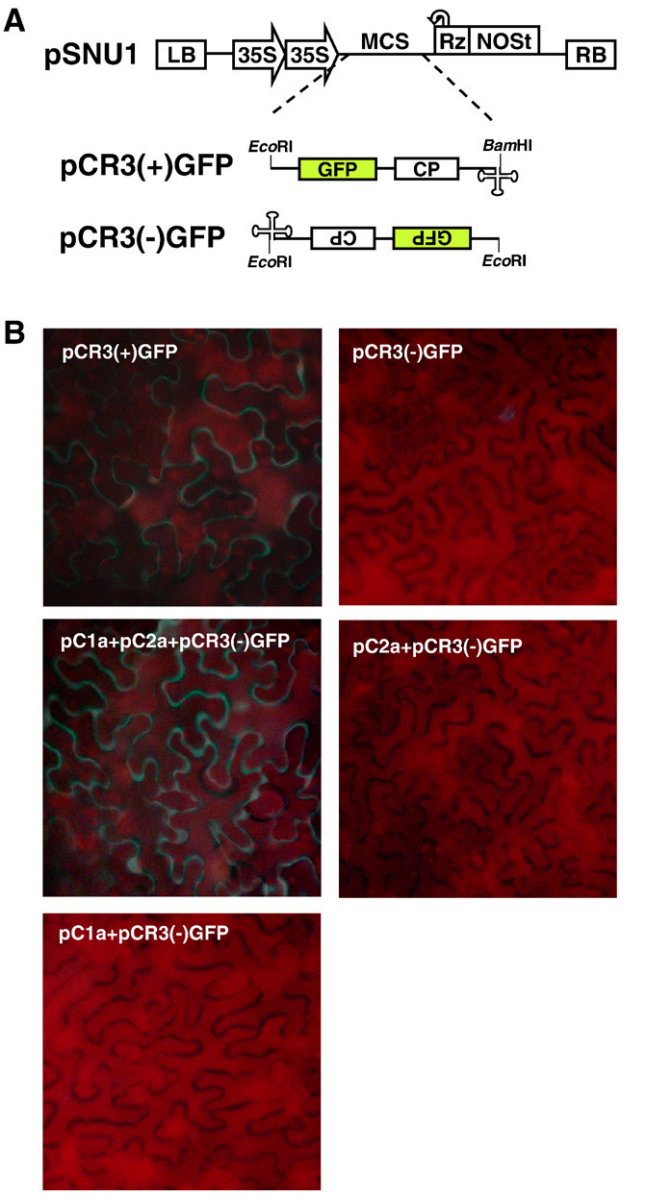

Fig. 5. Translatability of positive-strand RNA synthesized by 2a alone. (A) Schematic of pCR3(+)GFP and pCR3(−)GFP expressing positive-strand and negative-strand RNA3 derivatives, respectively, in which the 3a gene has been replaced by the GFP gene. (B) Representative images of *N. benthamiana* leaves agroinfiltrated with pCR3(−)GFP together with pC1a and/or pC2a. Combinations of the constructs infiltrated into *N. benthamiana* leaves are indicated at the top of each microscopic image. All micrographs were taken at 3 dpi.

Capping activities of 1a function independently of 2a

We next questioned whether 1a and 2a are both involved in the RNA capping reaction. In yeast expressing BMV 1a alone, 1a localizes to intracellular membranes and induces formation of spherical compartments, in which viral replication occurs (Chen and Ahlquist, 2000; Schwartz et al., 2002). Moreover, in the absence of 2a, 1a selectively increases *in vivo* stability of positive-strand RNA3 and is capable of recruiting RNA3 to a membrane-associated state (Janda and Ahlquist, 1998). As mentioned previously, a domain implicated in RNA capping is found in the N-terminal half of 1a. Thus, we examined whether CMV 1a alone is sufficient for the RNA capping reaction *in vivo*. To this end, we inoculated *N. benthamiana* with positive-strand CMV RNA transcripts, with or without a cap, generated by *in vitro* transcription. Since a cap is crucial for translation, we hypothesized that if 1a translated from a capped RNA1 transcript could process capping of uncapped RNA2 and RNA3 transcripts, plants inoculated with uncapped RNA2 and RNA3 transcripts together with capped RNA1 transcripts should be infected with CMV. To test this hypothesis, we mechanically inoculated *N. benthamiana* leaves with various combinations of CMV RNA transcripts. Experiments were carried out three times independently, comprising 114 plants in total (Table 1). Symptoms were observed over a period of 2 weeks following the inoculation, and RT-PCR was used to analyze total RNA extracted from upper non-inoculated leaves (data not shown). As expected, all 13 plants inoculated with a mixture of 1 μg each of capped RNA1, RNA2, and RNA3 transcripts showed typical CMV-induced symptoms, whereas none of the plants inoculated with a mixture of 1 μg each of uncapped RNA1, RNA2, and RNA3 transcripts exhibited stunting or any other symptoms characteristic of infection with CMV. All plants inoculated with a mixture of 1 μg each of capped RNA1 and RNA2, and uncapped RNA3 transcripts were also systemically infected with

Table 1
Infectivity of mixtures of capped and/or uncapped CMV RNA transcripts in plants

In vitro transcript[a]						Infectivity[b]			
m^7G-RNA1	m^7G-RNA2	m^7G-RNA3	RNA1	RNA2	RNA3	Exp.1	Exp.2	Exp.3	Total
+	+	+				3/3	5/5	5/5	13/13
+	+				+	3/3	5/5	5/5	13/13
	+	+	+			0/3	0/5	0/10	0/18
+				+	+	1/3	2/5	3/10	6/18
			+	+	+	0/3	0/5	0/5	0/13
	++	++	++			0/3	0/5	0/5	0/13
++				++	++	3/3	5/5	4/5	12/13
			++	++	++	0/3	0/5	0/5	0/13

[a] + and ++ indicate 1 and 5 μg of transcripts, respectively.
[b] Number of plants infected/number of plants mechanically inoculated with a mixture of transcripts.

CMV. In contrast, the inoculation of 1 μg of uncapped RNA1 transcripts mixed with 1 μg each of capped RNA2 and RNA3 transcripts did not produce any CMV infection in a total of 18 plants. Interestingly, however, out of 18 plants inoculated with 1 μg each of capped RNA1 and uncapped RNA2 and RNA3 transcripts, six plants were systemically infected with CMV (Table 1). To make sure that these CMV infections in the six plants were induced by 1a-mediated capping of uncapped RNA2 and RNA3 transcripts, we carried out subsequent experiments by inoculating plants with a mixture of RNA1, RNA2, and RNA3 transcripts. When plants were inoculated with 5 μg each of capped RNA1 and uncapped RNA2 and RNA3 transcripts, 12 of 13 plants exhibited typical symptoms. In contrast, none of the plants inoculated with 5 μg of uncapped RNA1 mixed with either capped RNA2 and RNA3 or uncapped RNA2 and RNA3 transcripts developed any local or systemic symptoms (Table 1). Overall, these results imply that 1a alone has capping activities and that neither interaction nor complex formation between 1a and 2a is necessary for the capping reaction, although more research is needed to determine whether 2a affects this activity in any other manner.

In vivo effects of CMV 1a mutations on virus replication

To further investigate the role of 1a in virus replication and to gain insight into the amino acids involved in the capping reaction and RNA synthesis, we constructed specific CMV 1a alanine-substituted mutations based on pCR1(+) and pC1a clones. We chose to substitute the H81 and K720 residues located in the capping and helicase-like domain of CMV 1a, respectively. These residues are some of the most conserved amino acids in alphaviruses, including BMV and SIN (Fig. 6A). Moreover, previous work has shown that corresponding mutants of BMV 1a and SIN nsP1 abolished either capping activities or the putative helicase activity of 1a, consequently blocking RNA replication (Ahola and Ahlquist, 1999; Ahola et al., 2000; Wang et al., 1996). Thus, we first tested the effects of CMV 1a mutants H81A and K720A on virus replication in plants to compare to those of other alphaviruses. CMV pCR1(+) and its mutant derivatives were delivered to *N. benthamiana* leaves together with pCR2(+) and pCR3(+) by agro-infiltration. At 4 dpi, infiltrated leaves were collected and used to extract total RNA. We then analyzed virus replication directly by Northern blotting to measure positive-strand accumulation (Fig. 6B). In plants expressing wt R1(+), strong signals were detected for positive-strand RNA species. In plants expressing R1(+) mutant H81A, accumulation of positive-strand RNAs was detectable at approximately 8.5% of the wt level. In contrast, there was no detectable positive-strand accumulation in plants expressing the R1(+) mutant K720A (the helicase domain mutant) as well as the minus-RNA1 control (data not shown), implying that helicase activity is required for initiating negative-strand RNA synthesis (Fig. 6B). When plants were simultaneously agroinfiltrated with both pCR1(+) mutants H81A and K720A to test possible complementation between these mutations, we could detect only very low levels of positive-strand RNAs similar to that observed using the R1(+) mutant H81A on its own, suggesting that no intragenic complementation between these two mutants occurred. These results were reproducible in three separate experiments and consistent with those of the corresponding BMV 1a mutants (Ahola et al., 2000). We also monitored these agroinfiltrated plants for 2 weeks after infiltration to examine whether RNA1 mutants could infect plants systemically. Interestingly, from three independent experiments, five of 20 plants expressing the R1(+) mutant H81A exhibited typical CMV-induced symptoms, although the appearance and development of symptoms was delayed by 7 to 10 days compared to those in wt controls (Table 2). In contrast, when plants were agroinfiltrated with pCR1(+) mutant K720A together with pCR2(+) and pCR3(+), no evidence of systemic infection was seen on

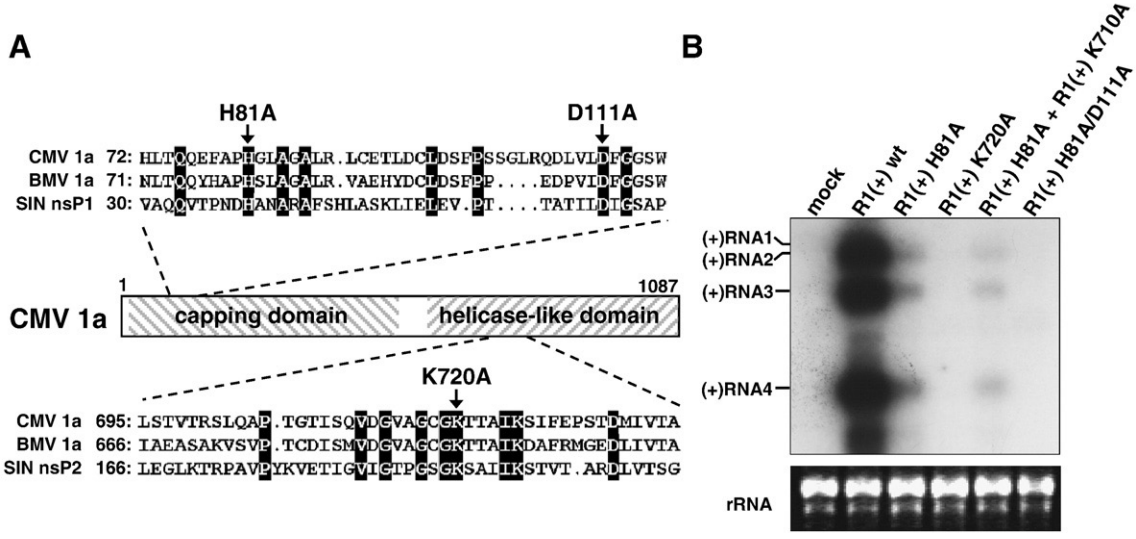

Fig. 6. Effects of 1a mutations on virus replication. (A) Schematic of CMV 1a and its alanine-substituted derivatives. The hatched boxes indicate capping and helicase-like domains of CMV 1a. The homologous regions shared by the different alphaviruses are identified by black boxes. The mutations used in this study are indicated by arrows at the top. (B) Northern blot analysis of RNA replication in plants infiltrated with pCR1(+) or its mutated derivatives together with pCR2(+) and pCR3(+). Total RNA was isolated from *N. benthamiana* leaves infiltrated with pCR2(+), pCR3(+), and either pCR1(+) or its derivatives indicated at the top of image. Northern blotting was performed using strand-specific probes to detect positive-strand CMV RNAs.

Table 2
Infectivity of CMV wt 1a or its mutated derivatives in plants

Agroinfiltration	Infectivity[a]			
+ R2(+) + R3(+)	Exp.1	Exp.2	Exp.3	Total
R1(+) wt	3/3	3/3	3/3	9/9
R1(+) H81A	1/4	1/6	3/10	5[b]/20
R1(+) H81A/D111A	0/4	0/6	0/10	0/20
R1(+) K720A	0/4	0/6	0/10	0/20
R1(−)	0/4	0/4	0/3	0/11
R1(−) +1a wt	4/4	4/4	3/3	11/11
R1(−) + 1a H81A	2/4	4/6	5/8	11[c]/18
R1(−) + 1a H81A/D111A	0/4	0/6	0/8	0/18
R1(−) + 1a K720A	4/4	6/6	8/8	18[d]/18

[a] Number of plants infected/number of plants infiltrated with a mixture of Agrobacterium cultures.
[b] All infected plants showed delayed symptom development.
[c] 6 of 11 infected plants showed delayed symptom development.
[d] 6 of 18 infected plants showed delayed symptom development.

upper leaves (Table 2). CMV infections were also confirmed by RT-PCR analysis using total RNA extracted from upper non-inoculated leaves (data not shown). Since the low fidelity of RdRp during virus replication may result in the restoration of viral RNA mutants (Rao and Hall, 1993), we analyzed progeny sequences of the R1(+) mutant H81A by RT-PCR using total RNA extracted from upper leaves of plants systemically infected with CMV. Sequence analysis of the progeny revealed that the amino acid substitution at position 81 was restored from alanine to histidine. These results were unexpected, since previous studies suggested that BMV 1a mutation H80A, which corresponds to the CMV 1a mutation H81A, disrupts the capping activities of 1a (Ahola and Ahlquist, 1999; Ahola et al., 2000). One of the possible reasons for this restoration of the CMV mutation may be due to differences between the two mutants. That is, CMV 1a mutation H81A might not be completely defective for capping activities, and hence may weakly support viral replication. To overcome this problem, we included a double mutation by combining mutation H81A with mutation D111A (Fig. 6A). CMV 1a mutation D111A is corresponding to BMV 1a mutation D106A, which is also defective for capping activities in BMV replication (Ahola et al., 2000). Thus, this double mutation should be more difficult to revert to wt sequence. When plants expressing the R1(+) mutant H81A/D111A were analyzed for the accumulation of positive-strand RNAs by Northern blotting, there was no detectable signal (Fig. 6B). Furthermore, none of the plants expressing this double mutation was infected with CMV (Table 2). This indicates that the CMV 1a double mutation H81A/D111A may be defective for capping activities, and thus not support detectable RNA replication.

Capping activities of CMV 1a function independently of helicase activity

Using the 1a mutations described above, we next examined whether CMV 1a could function in an RNA capping reaction despite a defect in helicase activity. To test this, we expressed CMV wt 1a protein or its mutant proteins in *N. benthamiana* leaves together with R1(−), R2(+), and R3(+) by agroinfiltration (Table 2). As demonstrated above, plants expressing R1(−), R2(+), and R3(+) could accumulate uncapped positive-strand RNA1. Simultaneous expression of mutant 1a protein in plants could mediate capping of uncapped positive-strand RNA1 encoding wt 1a. Therefore, if mutant 1a preserves its capping activities, plants expressing this mutant 1a together with R1 (−), R2(+), and R3(+) will be systemically infected with wt CMV. We carried out these experiments independently three times, and symptoms were observed over a period of 2 weeks following agroinfiltration. As expected, all plants expressing wt 1a together with R1(−), R2(+), and R3(+) developed typical symptoms, whereas none of the plants expressing R1(−), R2(+), and R3(+) alone exhibited any evidence of systemic infection. In the case of CMV 1a mutant H81A, 11 of 18 plants were systemically infected (six of 11 infected plants showed delayed symptom development), supporting that 1a mutant H81A maintains weak capping activities. On the other hand, none of the plants expressing CMV 1a mutant H81A/D111A, which is thought to be completely defective for capping activities, developed any symptoms. Moreover, expressing CMV 1a mutant K720A induced systemic infection in all plants tested (six of 18 infected plants showed delayed symptom development), suggesting that 1a mutant K720A preserves capping activities and that helicase activity is not necessary for RNA capping reaction.

Discussion

It is generally assumed that, in positive-strand RNA viruses, the accumulation of negative-strand RNA is significantly less than that of positive-strand RNA. For example, in BMV replication, positive-strand RNAs accumulate to a level greater than 100-fold that observed for negative-strand RNAs (French and Ahlquist, 1987; Marsh et al., 1991). We found similar strand accumulation asymmetry during CMV replication (Figs. 4C and D). Moreover, the kinetics of BMV and CMV RNA replication reveals that the synthesis of positive and negative strands is differently regulated (Figs. 4C and D; Kroner et al., 1990). In BMV, the rate of positive-strand accumulation is nearly linear until 20 h after inoculation, while negative-strand accumulation reaches a plateau 8 h after inoculation (Kroner et al., 1990). A model for temporal regulation of positive- and negative-strand RNA synthesis has been proposed in SIN (Lemm et al., 1994; Shirako and Strauss, 1994). Early in infection, uncleaved P123 and nsP4 of SIN form an initial replicase complex and function in negative-strand synthesis. By contrast, late in infection, when viral protein concentration is high, most P1234 are cleaved into nsP1, nsP2, nsP3, and nsP4. Under these conditions, negative-strand synthesis is shut off and the now stable replicase complex, which remains active throughout the infection cycle, switches to the synthesis of positive-strand and subgenomic RNAs. SIN nsP1 and nsP2 have enzyme activities corresponding to the N- and C-terminal halves of CMV 1a, respectively (Gorbalenya et al., 1989; Mi et al., 1989; van der Heijden and Bol, 2002). nsP4, which contains a viral RdRp domain, corresponds to CMV 2a (Kamer and Argos, 1984; van der Heijden and Bol, 2002). Furthermore, the roles and functions of these corresponding proteins have fundamental similarities in virus replication (Kao and Ahlquist, 1992; Schwartz et al., 2002; Shirako et al., 2000; Wang et al., 1991). Therefore, it is possible that alphaviruses including SIN, BMV, and CMV share common features of their replication strategies; specifically, the synthesis of positive- and negative-strand RNA is regulated by altering conformation or components of the replication complex.

In CMV, as well as BMV, complete RNA replication requires both 1a and 2a. A number of genetic studies suggest that 1a and 2a specifically interact to form a complex required for at least some steps in replication. As noted earlier, 1a and 2a cofractionated in active RdRp preparations and were coimmunoprecipitated with antisera to either 1a or 2a (Kao et al., 1992; Quadt and Jaspars, 1990). 1a and 2a also colocalize in intracellular membranes and form spherules, which are thought to be sites of virus replication (Chen and Ahlquist, 2000; Schwartz et al., 2002). Moreover, 1a plays crucial roles in recognizing positive-strand RNAs and recruiting these RNAs to a membrane-associated, nuclease-resistant state (Janda and Ahlquist, 1998; Wang et al., 2005). Taken together, these results strongly suggest that at least some proportion of 1a and 2a physically interacts. This physical interaction between 1a and 2a appears to be important for initiation of viral replication, especially for negative-strand synthesis. Consistent with previous results, we have shown here that without 1a or with either CMV 1a mutants K720A or H81A/D111A, RNA replication was abolished, likely due to interruption of the formation of a replicase complex competent for negative-strand synthesis (Figs. 2 and 6B).

Concomitantly, however, it appears that there are two forms of 2a in infected cells: 1a-associated 2a and cytoplasmic 2a, which is not associated with 1a (Chen and Ahlquist, 2000; Gal-On et al., 2000; Van Der Heijden et al., 2001). 2a is present not only in membrane fractions but also in the cytoplasm of infected cells, while 1a is entirely membrane-associated (Chen and Ahlquist, 2000; Gal-On et al., 2000; Van Der Heijden et al., 2001). Moreover, accumulation of phosphorylated 2a increases gradually in CMV-infected protoplasts (Kim et al., 2002). Interestingly, this phosphorylation of the CMV 2a prevents physical assembly of the 1a–2a complexes *in vitro* (Kim et al., 2002). Nevertheless, in the presence of 1a, most of 2a proteins nearly colocalize with 1a to intracellular membrane (Chen and Ahlquist, 2000; Cillo et al., 2002; Restrepo-Hartwig and Ahlquist, 1996; Schwartz et al., 2002). However, it is unlikely that all of these 2a proteins are membrane-associated by 1a because there are hundreds of 1a's per spherule and BMV 1a is present in approximately 25-fold excess over 2a in membrane fractions, especially, in spherules (Schwartz et al., 2002) while 2a is more abundant than 1a in CMV-infected tissues (Cillo et al., 2002; Gal-On et al., 1994). Recently, it was revealed that BMV 2a is concentrated in cytoplasmic foci (not diffuse freely throughout cytosol) even in the absence of 1a and these foci are often near or colocalized with cytoplasmic processing bodies (P bodies) (Beckham et al., 2007). It was also observed that BMV RNAs accumulate in P bodies in a manner dependent on cis-acting RNA replication signals in the absence of 1a (Beckham et al., 2007). Furthermore, previous studies have shown that Lsm1–7p complex, Dhh1p, and Pat1p, which are all components of P bodies, are required for viral complete replication and that a subpopulation of P bodies is associated with ER membrane in *Drosophila* oocytes, and multiple P body components in yeast co-fractionate with membranes (Beckham et al., 2007; Diez et al., 2000; Kushner et al., 2003; Mas et al., 2006; Noueiry et al., 2003; Wilhelm et al., 2005). In all, these suggest that more complicated subcellular structures beyond forming spherules or alternate interaction among replicase components may be implicated in viral replication.

In this study, we found that CMV 2a alone could synthesize positive-strand RNAs from negative-strand templates with similar activity compared to that observed in the presence of 1a (Figs. 2 and 4). Moreover, it is likely that no 1a activities participate in recognition of *cis*-acting sequences required for initiation of CMV positive-strand and subgenomic RNA synthesis (Fig. 3). Although we could not show whether 2a fraction, which is not associated with 1a, can synthesize positive-strand RNAs from negative-strand templates in the presence of wt 1a since effects of 1a for the positive-strand synthesis cannot be eliminated in this condition, we showed indirectly that CMV 2a can support the positive-strand RNA synthesis from negative-strand template in the presence of CMV 1a helicase mutant K720A corresponding to BMV 1a mutant K691A, which can recruit 2a to intracellular membrane and form spherules, but cannot recruit RNA3 to nuclease-resistant state and support RNA replication (Ahola et al., 2000; Wang et al., 2005, Table 2). Therefore, we suggest that CMV 2a, which is not associated with 1a, might be involved in synthesis of positive-strand RNAs in complete CMV replication. Consistently, deletion of the N-terminal region of BMV 2a, which is found to be important for interaction with 1a *in vitro* and *in vivo*, supported RNA replication at levels approaching those of wt 2a, while similar N-terminal deleted BMV 2a is concentrated in cytoplasmic punctuate spots even in the presence of 1a (Chen and Ahlquist, 2000; Kao and Ahlquist, 1992; Smirnyagina et al., 1996). In addition, as noted above, phosphorylated CMV 2a, which cannot interact with 1a, increases gradually, indicating that phosphorylation occurs late during the replication cycle. Accordingly, early in the replication cycle, formation of CMV 1a–2a complexes would not be prevented by phosphorylation, and these 1a–2a complexes may be involved in recruiting RNA replication templates and initiating negative-strand synthesis. The kinetics of CMV positive- and negative-strand RNA accumulation shows that the RNA replication was switched from negative-strand synthesis to positive-strand synthesis around 36 h after infection in plants (Figs. 4C and D). Furthermore, there is a large portion of 2a, not associated with 1a, in cytoplasm of plants at 72 h after infection and it was suggested that this cytoplasmic 2a may be phosphorylated (Gal-On et al., 2000; Kim et al., 2002). Therefore, while it has not been shown that phosphorylated CMV 2a maintains RdRp activity, we propose that it may play an important role in switching the function of 2a from negative-strand synthesis to positive-strand synthesis by dissociating 1a–2a complexes.

To further understand replication complex assembly, we investigated CMV 1a enzyme activities involved in RNA replication. We showed that CMV 1a is able to mediate capping of positive-strand RNAs in the absence of 2a, suggesting that interactions between 1a and 2a are not required for the capping reaction (Table 1). This result is consistent with the *in vitro* results of previous investigators who have shown that BMV 1a protein expressed in yeast or *Escherichia coli* forms a covalent complex with a guanine nucleotide and retains methyltransferase activity in the absence of other BMV components including 2a (Ahola and Ahlquist, 1999; Kong et al., 1999). Moreover, our *in vivo* results suggest that CMV 1a mutation K720A, which is thought to have a defect in helicase activity, preserves capping activities. Even though CMV 1a mutant K720A did not accumulate any detectable positive-strand RNA, this helicase mutant is likely capable of capping positive-strand RNAs (Fig. 6B and Table 2). Consistent with the above findings, other studies have shown that BMV 1a mutation K691A, corresponding to CMV 1a mutation K720A, is fully active in the covalent m^7GMP binding reaction and has 50% of the wt level of methyltransferase activity (Ahola and Ahlquist, 1999). It is noteworthy that BMV 1a mutation K691A is also defective for synthesis of both negative- and positive-strand RNA (Ahola et al., 2000). Therefore, it is likely that the helicase activity of 1a is not essential for the RNA capping reaction. Additionally, CMV 1a mutation K720A was completely unable to carry out positive-strand and subgenomic RNA synthesis (Fig. 6B). Since positive-strand RNA viruses replicate their genomes through negative-strand RNA intermediates, it is most likely that helicase activity is crucial for aspects of negative-strand RNA synthesis. Indeed, for poliovirus and bovine viral diarrhea virus as well as BMV, helicase activity appears to be required for initiation of negative-strand RNA synthesis (Barton and Flanegan, 1997; Gu et al., 2000; Kroner et al., 1990).

It was previously shown that BMV defective in capping activities can replicate in yeast strains devoid of *XRN1*, encoding the cap-sensitive 5′–3′ RNA exonuclease (Ahola et al., 2000). This implies that capping activities do not appear to be directly involved in RNA transcription of both positive and negative strands and that helicase activity can function independently of capping activities. The mutation H81A of CMV 1a was found to have a similar defect in viral RNA accumulation corresponding to a BMV mutant (Fig. 6B). However, CMV 1a mutation H81A can be restored to the wt sequence, likely due to its weak capping activities supporting leaky replication (Table 2). In contrast, CMV 1a double mutation H81A/D111A did not accumulate any detectable positive-strand RNA (Fig. 6B). This double mutation appears to completely disrupt capping activities, since none of the plants expressing CMV 1a mutant H81A/D111A together with R1(−), R2(+), and R3(+) was infected with CMV (Table 2). Additionally, since CMV 1a capping mutants synthesized severely reduced or undetectable levels of negative- as well as positive-strand RNAs (Fig. 6B; Ahola et al., 2000), it is possible that mutations in the capping domain may affect helicase activity and thereby disrupt functions of 1a involved in negative-strand synthesis. In all, it is likely that the capping and helicase activities can function separately and independently of each other in different steps of replication, even if their activity and efficiency are largely reduced. However, either molecular conformation or physical proximity between two 1a domains might be crucial for complete RNA replication, since complementation between CMV 1a mutation H81A and K720A was not observed.

Based on previous studies (Ahola et al., 2000; Beckham et al., 2007; Dinant et al., 1993; Gal-On et al., 1994; Kim et al., 2002; Kroner et al., 1990; Schwartz et al., 2002; Smirnyagina et al., 1996) and results presented here, we suggest a hypothetical model for temporal regulation of negative- and positive-strand CMV RNA synthesis by focusing on 1a–2a interactions (Fig. 7). Early in replication, 1a and 2a proteins, which are translated from positive-strand RNA1 and RNA2, respectively, colocalize on the intracellular membrane and interact to form spherules or vesicles. Positive-strand RNA templates are also recruited into the membrane-associated, nuclease-resistant state via interaction with 1a. In association with one or more host proteins, the 1a–2a complex functions as the active replicase for initiating negative-strand RNA synthesis. As 2a protein is phosphorylated by membrane-associated host kinases during the replication cycle, the formation of the 1a–2a complex is disrupted, leading to either a plateau or reduction in negative-strand accumulation. The phosphorylation of 2a now results in conversion of replicase activity from negative-strand synthesis to positive-strand synthesis. Since 1a and 2a proteins can function separately, the replicase comprising phosphorylated 2a and some host proteins initiate positive-strand RNA synthesis, and 1a independently processes capping reactions after transcription. Eventually, accumulation of progeny positive-strand RNAs increases late during replication.

In this study, we focused on dissecting the interactions of viral replicase activities in positive- and negative-strand synthesis. Our results revealed only a small fraction of the possible scenarios for temporal regulation of 1a–2a interactions in CMV replication. Crucial details remain to be elucidated for replication complex assembly including the association and contribution of various host proteins in the replication cycle. Accumulating evidence indicates that host proteins play an important role in positive-strand RNA virus replication, including assembly of the replicase complex, targeting of the complex to intracellular membranes, recruiting RNA templates, regulating replicase activities, and other processes (reviewed in reference Ahlquist et al., 2003). It is clear that varied genetic and biochemical approaches will be needed for characterizing viral replication complexes and identifying host proteins and their roles in RNA replication.

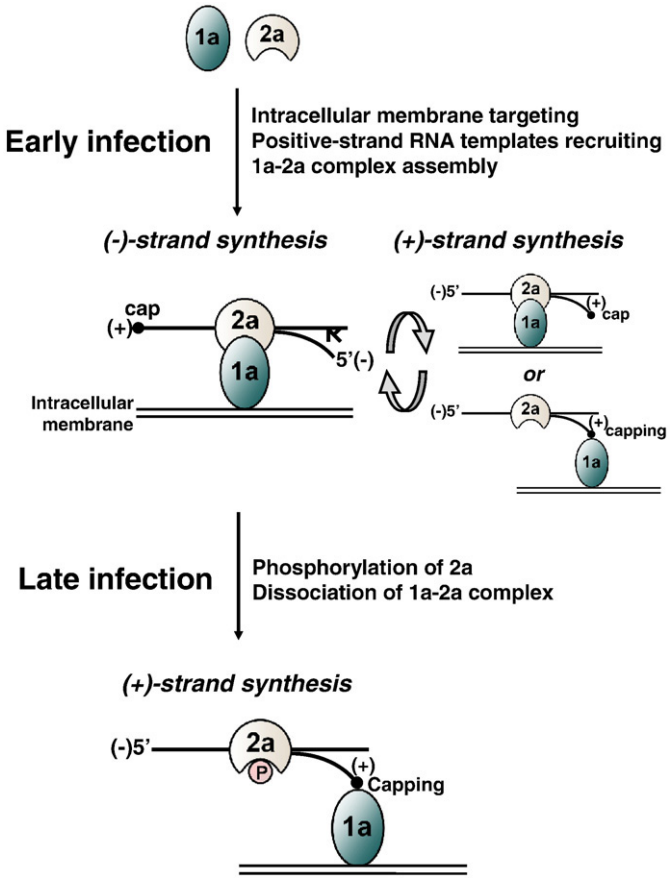

Fig. 7. Model for the temporal regulation of negative- and positive-strand RNA synthesis. See Discussion for details.

Materials and methods

Plasmid construction

To develop a DNA-based transient expression system to express CMV RNAs for replication and infection in plants, each full-length cDNA of CMV strain Fny was amplified using various pairs of primers containing the appropriate restriction sites (Table 3). These were cloned in either the forward or reverse orientation into the T-DNA region of a modified binary vector, pSNU1, derived from pCAMBIA0390 as described previously (Liu et al., 2002; Park and Kim, 2006). The resulting plasmids were designated pCR1(+), pCR1(−), pCR2(+), pCR3(+), and pCR3(−) corresponding to the CMV cDNAs and their orientations (Fig. 1). RNA2 and RNA3 deletion mutants were constructed by deleting either the 5′- or 3′-terminal sequences, amplified using appropriate pairs of primers (Table 3), and cloned into pSNU1. The resulting deletion mutants were named pCR3(−)Δ3, pCR3(−)Δ5, pCR4(−), pCR4(−)Δpro, pCR4A(−), and pCR4A(−)Δpro (Fig. 3A). To express CMV proteins from replication-incompetent RNAs, cDNAs encoding 1a and 2a sequences were amplified and fused onto the downstream leader sequence from tobacco etch virus by double-joint PCR using corresponding primer pairs (Table 3) as described previously (Yu et al., 2004). The PCR fragments were cloned into a modified pSNU1 vector. The resultant plasmids, pC1a and pC2a, contain, in sequential order, a double 35S promoter, TEV leader sequence, either 1a or 2a coding sequence, and a NOS terminator (Fig. 1). To make pR3(−)GFP, the 3a coding sequence from a version of pCR3(−) was replaced with the sequence coding for GFP. GFP was amplified using a pair of primers (Table 3) that contain KpnI restriction sites. The PCR products were digested with KpnI to exclude the 3a coding region and cloned into pCR3(−). Alanine-substituted 1a derivatives H81A, D111A, and K720A were constructed based on both pCR1(+) and pC1a, respectively. Alanine-substitution was carried out by PCR-based, site-directed mutagenesis using mismatched primers (Table 3) as described elsewhere (Nassal and Rieger, 1990). Plasmids containing full-length cDNAs of CMV-Fny adjacent to a T7 promoter sequence were obtained from the Plant Virus Gene Bank at Seoul Women's University. The sequences of all constructs were validated by DNA sequencing using the dideoxynucleotide termination method and an ABI Prism 3730 XL DNA Analyzer (Applied Biosystems, USA).

In vitro transcription and transcript inoculation

Prior to *in vitro* transcription, each CMV cDNA clone was linearized by cleavage with appropriate restriction enzymes: PstI for positive-strand RNA1, RNA2, and RNA3 transcription clones, SpeI for negative-strand RNA1 and RNA3 transcription clones. The 3′ overhang of PstI-linearized template DNA was removed with T4 DNA polymerase (NEB, USA). The linearized plasmids were transcribed using the MEGAscript® T7 kit (Ambion, USA) and RNA cap structure analog (NEB, USA) according to the manufacturers' instructions. All transcripts obtained by *in vitro* transcription were treated with TURBO DNA-*free*™ (Ambion, USA) to remove DNA contamination according to the manufacturer's instructions. Equal volumes of transcripts were combined and gently rubbed onto plant leaves with carborundum.

Agroinfiltration

Agroinfiltration into *N. benthamiana* was carried out as described previously (Koscianska et al., 2005) with some modifications. Briefly, All

T-DNA constructs were introduced into *Agrobacterium* strain GV2260 by electroporation. Agrobacteria harboring each plasmid were grown at 30 °C overnight in YEP medium with kanamycin (50 μg/mL) and acetosyringon (20 μM). The cultures were centrifuged at 4000 rpm for 10 min, and the pellets were resuspended in infiltration medium (MS salts, 10 mM MES, pH 5.6, 200 μM acetosyringon) and incubated at 30 °C for a minimum of 2 h. *Agrobacterium* cultures (at 0.5 OD_{600}) were mixed in equal proportions prior to infiltration and were infiltrated onto the abaxial surface of leaves at the four-to-five leaf stage using a 1-ml syringe. After agroinfiltration, the plants were kept in constant conditions at 25 °C-day and 22 °C-night with a 16-h photoperiod.

Total RNA extraction

Total RNA was prepared using the TRI Reagent method (MRC, USA) and further treated with TURBO DNA-*free*™ (Ambion, USA) according to the manufacturer's instructions.

Strand-specific RT-PCR

Strand-specific RT-PCR was carried out as described previously (Lanford et al., 1994; Lin et al., 2002) with some modifications. Briefly, total RNA was denatured at 95 °C for 5 min with 10 μM of appropriately tagged RT primer: prR1(+)T-Rv, prR3(+)T-Rv, prR3(−)T-Rv, prCP(+)T-Rv, or prR4A(+)T-Rv (Table 3). Each tagged RT primer contains a non-CMV sequence (tag, boldface) at the 5′ end and a CMV sequence at the 3′ end. The RT reaction was incubated at 55 °C for 30 min with 200U of SuperScript™ III (Invitrogen, USA), followed by heat inactivation at 99 °C for 1 h. The resulting cDNA was purified using a GENECLEAN® *Turbo* kit (Qbiogene, USA) to remove residual RT primer. The cDNA was amplified by 30 cycles of hot start PCR using *Pfu* polymerase (iNtRON, Korea) and 10 μM of each primer: prTAG (tag sequence) and either prR1(+)-Fw, prR3(+)-Fw, prR3(−)-Fw, prCP(+)-Fw, or prR4A(+)-Fw (Table 3). After initial denaturation at 94 °C for 5 min, each cycle consisted of 30 s at 94 °C, 20 s at 60 °C, and 60 s at 72 °C. PCR products were analyzed by agarose gel electrophoresis.

Northern blot analysis

Northern blots were performed as described previously (Lee et al., 2004). Briefly, 20 μg of total RNA was fractionated by electrophoresis and transferred to positively charged nylon membranes (Amersham, UK). Hybridization was carried out using ULTRAhyb®-Oligo hybridization buffer (Ambion, USA) and ^{32}P end-labeled DNA oligonucleotide

Table 3
Primers used in this study

Name	Sequence	Purpose
R1,2 5′End-EcoRI	GGAATTCGTTTATTTACAAGAGCGTACGG	To construct pCR1(+), pCR1(−),
R1,2 5′End-BamHI	AGGGATCCGTTTATTTACAAGAGCGTACGG	pCR2(+), pCR3(+), and pCR3(−)
R3 5′End-EcoRI	GGAATTCGTAATCTTACCACTGTG	
R3 5′End-BamHI	AGGGATCCGTAATCTTACCACTGTG	
RNA 3′End-EcoRI	GGAATTCTGGTCTCCTTTTRGAGRCC	
RNA 3′End-BamHI	AGGGATCCTGGTCTCCTTTTRGAGRCC	
R3(−) Fw102-BamHI	AGGGATCCTCGTGTTGTCCGCACATTTG	To construct pCR3(−)Δ3,
R3(−) Rv2176-BamHI	AGGGATCCTAGGAGATGGTTTCAAAGG	pCR3(−)Δ5, pCR4(−), pCR4(−)Δpro,
R3(−) Rv1131-BamHI	AGGGATCCTCTGGTTTTAGTAAGCCTACATCA	pCR4A(−), and pCR4A(−)Δpro
R3(−) Rv1015-BamHI	AGGGATCCATAGAGAGTGTTTGTGCT	
R2 2319 Fw-BamHI	AGGGATCCTCTATTATTCAGATCGTC	
R2 2360 Fw-BamHI	AGGGATCCGTTTTGTAGTACAGAGTTCA	
TEV-L Fw-BamHI	AGGGATCCAATTCTCAACACAACATATA	To construct pC1a and pC2a
TEV-1a DJ	TTGAACGAGGACGTCGCCATGGCTATCGTTCGTAAATGGT	
TEV-2a DJ	TGCGGGGGCAGGGAAAGCCATGGCTATCGTTCGTAAATGGT	
CMV 1a Rv	CTAAGCACGAGCAACACATT	
CMV 2a Rv	TCAGACTCGGGTAACTCCG	
GFP Fw-KpnI	GGGGTACCAGTAAAGGAGAAGAACTTTTCA	To amplify GFP
GFP Rv-KpnI	GGGGTACCCTATTTGTATAGTTCATCCATGC	
R1 H81A Fw	GTTTGCTCCCGCCGGCCTAGCTGGT	To construct 1a
R1 D111A Rv	TCCTCCGAAGGCTAAGACGAG	alanine-substituted mutants
R1 K720A Rv	TAATTGCCGTGGTTGCCCCA	
prR1(+)T-Rv	**GCTGGAATTCGCGGTTAAA**TCACACTAGCGATGGCACGAGATG	For strand-specific RT-PCR
prR1(+)-Fw	GCGGGCGGTGATGACAAAAG	(for positive-strand RNA1;
prR3(+)T-Rv	**GCTGGAATTCGCGGTTAAA**CAACTCAGATCCCGCCACAGA	prR1(+)T-Rv and prR1(+)-Fw,
prR3(+)-Fw	TCCCTGTTGAGCCCCCTTACTTT	for positive-strand RNA3;
prR3(−)T-Rv	**GCTGGAATTCGCGGTTAAA**TCCCTGTTGAGCCCCCTTACTTT	prR3(+)T-Rv and prR3(+)-Fw,
prR3(−)-Fw	CAACTCAGATCCCGCCACAGA	for negative-strand RNA3;
prCP(+)T-Rv	**GCTGGAATTCGCGGTTAAA**CAGATGTGGGAATGCGTTGGT	prR3(−)T-Rv and prR3(−)-Fw,
prCP(+)-Fw	CGTCGTCCGCGTCGTGGTT	for positive-strand RNA4;
prR4A(+)T-Rv	**GCTGGAATTCGCGGTTAAA**CACCCGTACCCTGAAACTA	prCP(+)T-Rv and prCP(+)-Fw
prR4A(+)-Fw	TGAACGTAGGTGCAATGAC	for positive-strand RNA4A;
prTAG	GCTGGAATTCGCGGTTAAA	prR4A(+)T-Rv and prR4A(+)-Fw)
CMV R1(+) probe	AATCCCCAAAACATATAGCTCGCACGGCCTTCAACT	For northern blotting
CMV R3(+) probe	CAGATGTGGGAATGCGTTGGTGCTCGATGTCA	
CMV R3(−) probe	TGACATCGAGCACCAACGCATTCCCACATCTG	
CMV 123(+) probe	GGCACCCGTACCCTGAAACTAGCACGTTGTG	
prR3-RT Fw	TGGGCAATGCGTTTCGTTA	For real-time RT-PCR
prR3-RT Rv	CCGCTTACGATTCCCAACTG	(pr3 3′E Rv was used for RT
prR4-RT Fw	TCCTTTGCCGAAATTTGATTCT	of positive-strand RNA3.
prR4-RT Rv	GTCCGCGAACATAGCAGAGAT	Oligo(dT)18 was used for RT
prR3 3′E Rv	TGGTCTCCTTTTGGAGGCC	of ubiquitin mRNA.)
prUbi-RT Fw	GCCGACTACAACATCCAGAAGG	
prUbi-RT Rv	TGCAACACAGCGAGCTTAACC	
Oligo(dT)18	TTTTTTTTTTTTTTTT	

The restriction enzyme sites are underlined.
The mutated sequences for alanine substitution are underlined and written in italics.
The non-CMV sequences (tag) are shown boldface.

probes (Table 3; for positive-strand RNA1 detection, CMV R1(+) probe; for positive-strand RNA3 detection, CMV R3(+) probe; for negative-strand RNA3 detection, CMV R3(−) probe; for CMV positive-strands detection, CMV 123(+) probe) according to the manufacturer's protocol.

Western blot analysis

Total protein extraction from *N. benthamiana* leaves was performed using the TRI Reagent method (MRC, Cincinnati, OH) according to the manufacturer's instructions. Protein concentration was estimated by the Bradford assay. Total proteins were separated by 12% SDS-PAGE and transferred onto PVDF transfer membranes. The blots were probed with antibodies against CMV 3a or CP (Plant Virus Gene Bank, Korea). A secondary antibody, conjugated to horseradish peroxidase, was used with ECL chemiluminescent detection reagents (Amersham, UK) to visualize the antigens.

Real-time RT-PCR

Real-time RT-PCR was performed using Power SYBR® Green PCR Master Mix (Applied Biosystems, USA) and a 7500 Real Time PCR System (Applied Biosystems, USA) according to the manufacturer's instructions. The thermal profile was 50 °C for 2 min, 95 °C for 10 min, followed by 40 cycles of 95 °C for 15 s and 60 °C for 1 min. Primers were designed using Primer Express 3.0 software (Applied Biosystems, USA): prR3-RT-Fw and prR3-RT-Rv for positive-strand RNA3 detection, prR4-RT-Fw and prR4-RT-Rv for positive-strand RNA3 and RNA4 detection, and prUbi-RT-Fw and prUbi-RT-Rv for *ubiquitin* mRNA detection (Table 3). The *ubiquitin* gene was used as a housekeeping gene to standardize the different samples. Total RNA from plants infiltrated with pCR3(−)Δ5 alone was used to compensate for false positive signals.

Fluorescence microscopy

GFP signals from infiltrated leaf samples were visualized and photographed by fluorescence microscopy using a Carl Zeiss DE/Axioplan II microscope with a GFP filter set at 390- to 420-nm excitation and 450-nm emission parameters.

Acknowledgments

This research was supported in part by grants from the Korea Science and Engineering Foundation (KOSEF) grant (500-20080101) funded by the Korea government (MEST); the Agriculture Specific Research Project (500-20080083) funded by the Rural Development Administration; the BioGreen21 Program (500-20080113), Rural Development Administration to KHK; and by a Korea Research Foundation Grant funded by the Korean Government (MOEHRD, Basic Research Promotion Fund) (KRF-2005-217-F00001) to SJK. JKS was supported by graduate fellowship from the Ministry of Education through the Brain Korea 21 Project.

References

Ahlquist, P., Noueiry, A.O., Lee, W.M., Kushner, D.B., Dye, B.T., 2003. Host factors in positive-strand RNA virus genome replication. J. Virol. 77, 8181–8186.
Ahola, T., Ahlquist, P., 1999. Putative RNA capping activities encoded by brome mosaic virus: methylation and covalent binding of guanylate by replicase protein 1a. J. Virol. 73, 10061–10069.
Ahola, T., den Boon, J.A., Ahlquist, P., 2000. Helicase and capping enzyme active site mutations in brome mosaic virus protein 1a cause defects in template recruitment, negative-strand RNA synthesis, and viral RNA capping. J. Virol. 74, 8803–8811.
Allison, R.F., Janda, M., Ahlquist, P., 1988. Infectious in vitro transcripts from cowpea chlorotic mottle virus cDNA clones and exchange of individual RNA components with brome mosaic virus. J. Virol. 62, 3581–3588.
Annamalai, P., Rao, A.L., 2005. Replication-independent expression of genome components and capsid protein of brome mosaic virus in planta: a functional role for viral replicase in RNA packaging. Virology 338, 96–111.
Barton, D.J., Flanegan, J.B., 1997. Synchronous replication of poliovirus RNA: initiation of negative-strand RNA synthesis requires the guanidine-inhibited activity of protein 2C. J. Virol. 71, 8482–8489.
Beckham, C.J., Light, H.R., Nissan, T.A., Ahlquist, P., Parker, R., Noueiry, A., 2007. Interactions between brome mosaic virus RNAs and cytoplasmic processing bodies. J. Virol. 81, 9759–9768.
Boccard, F., Baulcombe, D., 1993. Mutational analysis of cis-acting sequences and gene function in RNA3 of cucumber mosaic virus. Virology 193, 563–578.
Chen, J., Ahlquist, P., 2000. Brome mosaic virus polymerase-like protein 2a is directed to the endoplasmic reticulum by helicase-like viral protein 1a. J. Virol. 74, 4310–4318.
Chen, M.H., Roossinck, M.J., Kao, C.C., 2000. Efficient and specific initiation of subgenomic RNA synthesis by cucumber mosaic virus replicase in vitro requires an upstream RNA stem-loop. J. Virol. 74, 11201–11209.
Choi, S.K., Hema, M., Gopinath, K., Santos, J., Kao, C., 2004. Replicase-binding sites on plus- and minus-strand brome mosaic virus RNAs and their roles in RNA replication in plant cells. J. Virol. 78, 13420–13429.
Cillo, F., Roberts, I.M., Palukaitis, P., 2002. In situ localization and tissue distribution of the replication-associated proteins of Cucumber mosaic virus in tobacco and cucumber. J. Virol. 76, 10654–10664.
Diez, J., Ishikawa, M., Kaido, M., Ahlquist, P., 2000. Identification and characterization of a host protein required for efficient template selection in viral RNA replication. Proc. Natl. Acad. Sci. U. S. A. 97, 3913–3918.
Dinant, S., Janda, M., Kroner, P.A., Ahlquist, P., 1993. Bromovirus RNA replication and transcription require compatibility between the polymerase- and helicase-like viral RNA synthesis proteins. J. Virol. 67, 7181–7189.
Ding, S.W., Shi, B.J., Li, W.X., Symons, R.H., 1996. An interspecies hybrid RNA virus is significantly more virulent than either parental virus. Proc. Natl. Acad. Sci. U. S. A. 93, 7470–7474.
French, R., Ahlquist, P., 1987. Intercistronic as well as terminal sequences are required for efficient amplification of brome mosaic virus RNA3. J. Virol. 61, 1457–1465.
Gal-On, A., Kaplan, I., Roossinck, M.J., Palukaitis, P., 1994. The kinetics of infection of zucchini squash by cucumber mosaic virus indicate a function for RNA 1 in virus movement. Virology 205, 280–289.
Gal-On, A., Canto, T., Palukaitis, P., 2000. Characterisation of genetically modified cucumber mosaic virus expressing histidine-tagged 1a and 2a proteins. Arch. Virol. 145, 37–50.
Gallie, D.R., 1991. The cap and poly(A) tail function synergistically to regulate mRNA translational efficiency. Genes Dev. 5, 2108–2116.
Gopinath, K., Kao, C.C., 2007. Replication-independent long-distance trafficking by viral RNAs in *Nicotiana benthamiana*. Plant Cell 19, 1179–1191.
Gopinath, K., Dragnea, B., Kao, C., 2005. Interaction between Brome mosaic virus proteins and RNAs: effects on RNA replication, protein expression, and RNA stability. J. Virol. 79, 14222–14234.
Gorbalenya, A.E., Koonin, E.V., Donchenko, A.P., Blinov, V.M., 1989. Two related superfamilies of putative helicases involved in replication, recombination, repair and expression of DNA and RNA genomes. Nucleic Acids Res. 17, 4713–4730.
Gu, B., Liu, C., Lin-Goerke, J., Maley, D.R., Gutshall, L.L., Feltenberger, C.A., Del Vecchio, A.M., 2000. The RNA helicase and nucleotide triphosphatase activities of the bovine viral diarrhea virus NS3 protein are essential for viral replication. J. Virol. 74, 1794–1800.
Hayes, R.J., Buck, K.W., 1990. Complete replication of a eukaryotic virus RNA in vitro by a purified RNA-dependent RNA polymerase. Cell 63, 363–368.
Janda, M., Ahlquist, P., 1998. Brome mosaic virus RNA replication protein 1a dramatically increases in vivo stability but not translation of viral genomic RNA3. Proc. Natl. Acad. Sci. U. S. A. 95, 2227–2232.
Kamer, G., Argos, P., 1984. Primary structural comparison of RNA-dependent polymerases from plant, animal and bacterial viruses. Nucleic Acids Res. 12, 7269–7282.
Kao, C.C., Ahlquist, P., 1992. Identification of the domains required for direct interaction of the helicase-like and polymerase-like RNA replication proteins of brome mosaic virus. J. Virol. 66, 7293–7302.
Kao, C.C., Quadt, R., Hershberger, R.P., Ahlquist, P., 1992. Brome mosaic virus RNA replication proteins 1a and 2a form a complex in vitro. J. Virol. 66, 6322–6329.
Kim, S.H., Palukaitis, P., Park, Y.I., 2002. Phosphorylation of cucumber mosaic virus RNA polymerase 2a protein inhibits formation of replicase complex. EMBO J. 21, 2292–2300.
Kong, F., Sivakumaran, K., Kao, C., 1999. The N-terminal half of the brome mosaic virus 1a protein has RNA capping-associated activities: specificity for GTP and S-adenosylmethionine. Virology 259, 200–210.
Koonin, E.V., Dolja, V.V., 1993. Evolution and taxonomy of positive-strand RNA viruses: implications of comparative analysis of amino acid sequences. Crit. Rev. Biochem. Mol. Biol. 28, 375–430.
Koscianska, E., Kalantidis, K., Wypijewski, K., Sadowski, J., Tabler, M., 2005. Analysis of RNA silencing in agroinfiltrated leaves of *Nicotiana benthamiana* and *Nicotiana tabacum*. Plant Mol. Biol. 59, 647–661.
Kroner, P.A., Young, B.M., Ahlquist, P., 1990. Analysis of the role of brome mosaic virus 1a protein domains in RNA replication, using linker insertion mutagenesis. J. Virol. 64, 6110–6120.
Kushner, D.B., Lindenbach, B.D., Grdzelishvili, V.Z., Noueiry, A.O., Paul, S.M., Ahlquist, P., 2003. Systematic, genome-wide identification of host genes affecting replication of a positive-strand RNA virus. Proc. Natl. Acad. Sci. U. S. A. 100, 15764–15769.
Lanford, R.E., Sureau, C., Jacob, J.R., White, R., Fuerst, T.R., 1994. Demonstration of in vitro infection of chimpanzee hepatocytes with hepatitis C virus using strand-specific RT/PCR. Virology 202, 606–614.
Lee, J.J., Eisenberg, P., Papadopoulos, V., Wang, J., Widmaier, E.P., 2004. Reversible changes in adrenocorticotropin (ACTH)-induced adrenocortical steroidogenesis and expression of the peripheral-type benzodiazepine receptor during the ACTH-insensitive period in young rats. Endocrinology 145, 2165–2173.

Lemm, J.A., Rumenapf, T., Strauss, E.G., Strauss, J.H., Rice, C.M., 1994. Polypeptide requirements for assembly of functional Sindbis virus replication complexes: a model for the temporal regulation of minus- and plus-strand RNA synthesis. EMBO J. 13, 2925–2934.

Lin, L., Fevery, J., Hiem Yap, S., 2002. A novel strand-specific RT-PCR for detection of hepatitis C virus negative-strand RNA (replicative intermediate): evidence of absence or very low level of HCV replication in peripheral blood mononuclear cells. J. Virol. Methods 100, 97–105.

Liu, Y., Schiff, M., Marathe, R., Dinesh-Kumar, S.P., 2002. Tobacco Rar1, EDS1 and NPR1/NIM1 like genes are required for N-mediated resistance to tobacco mosaic virus. Plant J. 30, 415–429.

Marsh, L.E., Huntley, C.C., Pogue, G.P., Connell, J.P., Hall, T.C., 1991. Regulation of (+):(−)-strand asymmetry in replication of brome mosaic virus RNA. Virology 182, 76–83.

Mas, A., Alves-Rodrigues, I., Noueiry, A., Ahlquist, P., Diez, J., 2006. Host deadenylation-dependent mRNA decapping factors are required for a key step in brome mosaic virus RNA replication. J. Virol. 80, 246–251.

Mi, S., Durbin, R., Huang, H.V., Rice, C.M., Stollar, V., 1989. Association of the Sindbis virus RNA methyltransferase activity with the nonstructural protein nsP1. Virology 170, 385–391.

Nassal, M., Rieger, A., 1990. PCR-based site-directed mutagenesis using primers with mismatched 3′-ends. Nucleic Acids Res. 18, 3077–3078.

Noueiry, A.O., Diez, J., Falk, S.P., Chen, J., Ahlquist, P., 2003. Yeast Lsm1p–7p/Pat1p deadenylation-dependent mRNA-decapping factors are required for brome mosaic virus genomic RNA translation. Mol. Cell. Biol. 23, 4094–4106.

Palukaitis, P., Garcia-Arenal, F., 2003. Cucumoviruses. Adv. Virus Res. 62, 241–323.

Park, S., Kim, K., 2006. Agroinfiltration-based potato virus X replicons to dissect the requirements of viral infection. Plant Pathol. J. 22, 386–390.

Quadt, R., Jaspars, E.M., 1990. Purification and characterization of brome mosaic virus RNA-dependent RNA polymerase. Virology 178, 189–194.

Rao, A.L., Hall, T.C., 1993. Recombination and polymerase error facilitate restoration of infectivity in brome mosaic virus. J. Virol. 67, 969–979.

Restrepo-Hartwig, M.A., Ahlquist, P., 1996. Brome mosaic virus helicase- and polymerase-like proteins colocalize on the endoplasmic reticulum at sites of viral RNA synthesis. J. Virol. 70, 8908–8916.

Restrepo-Hartwig, M., Ahlquist, P., 1999. Brome mosaic virus RNA replication proteins 1a and 2a colocalize and 1a independently localizes on the yeast endoplasmic reticulum. J. Virol. 73, 10303–10309.

Schwartz, M., Chen, J., Janda, M., Sullivan, M., den Boon, J., Ahlquist, P., 2002. A positive-strand RNA virus replication complex parallels form and function of retrovirus capsids. Mol. Cell 9, 505–514.

Shirako, Y., Strauss, J.H., 1994. Regulation of Sindbis virus RNA replication: uncleaved P123 and nsP4 function in minus-strand RNA synthesis, whereas cleaved products from P123 are required for efficient plus-strand RNA synthesis. J. Virol. 68, 1874–1885.

Shirako, Y., Strauss, E.G., Strauss, J.H., 2000. Suppressor mutations that allow sindbis virus RNA polymerase to function with nonaromatic amino acids at the N-terminus: evidence for interaction between nsP1 and nsP4 in minus-strand RNA synthesis. Virology 276, 148–160.

Sivakumaran, K., Kao, C.C., 1999. Initiation of genomic plus-strand RNA synthesis from DNA and RNA templates by a viral RNA-dependent RNA polymerase. J. Virol. 73, 6415–6423.

Sivakumaran, K., Kim, C.H., Tayon Jr., R., Kao, C.C., 1999. RNA sequence and secondary structural determinants in a minimal viral promoter that directs replicase recognition and initiation of genomic plus-strand RNA synthesis. J. Mol. Biol. 294, 667–682.

Sivakumaran, K., Bao, Y., Roossinck, M.J., Kao, C.C., 2000. Recognition of the core RNA promoter for minus-strand RNA synthesis by the replicases of Brome mosaic virus and Cucumber mosaic virus. J. Virol. 74, 10323–10331.

Sivakumaran, K., Chen, M.H., Roossinck, M.J., Kao, C.C., 2002. Core prooter for initiation of cucumber mosaic virus subgenomic RNA4A. Mol. Plant Pathol. 3, 43–52.

Smirnyagina, E., Lin, N.S., Ahlquist, P., 1996. The polymerase-like core of brome mosaic virus 2a protein, lacking a region interacting with viral 1a protein in vitro, maintains activity and 1a selectivity in RNA replication. J. Virol. 70, 4729–4736.

Sonenberg, N., Trachsel, H., Hecht, S., Shatkin, A.J., 1980. Differential stimulation of capped mRNA translation in vitro by cap binding protein. Nature 285, 331–333.

Symons, R.H., 1975. Cucumber mosaic virus RNA contains 7-methyl guanosine at the 5′-terminus of all four RNA species. Mol. Biol. Rep. 2, 277–285.

van der Heijden, M.W., Bol, J.F., 2002. Composition of alphavirus-like replication complexes: involvement of virus and host encoded proteins. Arch. Virol. 147, 875–898.

Van Der Heijden, M.W., Carette, J.E., Reinhoud, P.J., Haegi, A., Bol, J.F., 2001. Alfalfa mosaic virus replicase proteins P1 and P2 interact and colocalize at the vacuolar membrane. J. Virol. 75, 1879–1887.

Wang, Y.F., Sawicki, S.G., Sawicki, D.L., 1991. Sindbis virus nsP1 functions in negative-strand RNA synthesis. J. Virol. 65, 985–988.

Wang, H.L., O'Rear, J., Stollar, V., 1996. Mutagenesis of the Sindbis virus nsP1 protein: effects on methyltransferase activity and viral infectivity. Virology 217, 527–531.

Wang, X., Lee, W.M., Watanabe, T., Schwartz, M., Janda, M., Ahlquist, P., 2005. Brome mosaic virus 1a nucleoside triphosphatase/helicase domain plays crucial roles in recruiting RNA replication templates. J. Virol. 79, 13747–13758.

Wilhelm, J.E., Buszczak, M., Sayles, S., 2005. Efficient protein trafficking requires trailer hitch, a component of a ribonucleoprotein complex localized to the ER in *Drosophila*. Dev. Cell 9, 675–685.

Yu, J.H., Hamari, Z., Han, K.H., Seo, J.A., Reyes-Dominguez, Y., Scazzocchio, C., 2004. Double-joint PCR: a PCR-based molecular tool for gene manipulations in filamentous fungi. Fungal Genet. Biol. 41, 973–981.